

Surfactant-Free Controlled/Living Radical Emulsion (Co)polymerization of *n*-Butyl Acrylate and Methyl Methacrylate via RAFT Using Amphiphilic Poly(ethylene oxide)-Based Trithiocarbonate Chain Transfer Agents

Jutta Rieger,^{†‡} Gregor Osterwinter,^{†‡} Chuong Bui,^{†‡} François Stoffelbach,^{†‡} and Bernadette Charleux^{*,†‡}

[†]UPMC Univ. Paris 6 and [‡]CNRS Univ. Paris 6, UMR 7610 Laboratoire de Chimie des Polymères, 4 Place Jussieu, Tour 44-54, 75252 Paris Cedex 05, France

Received April 22, 2009; Revised Manuscript Received June 7, 2009

ABSTRACT: The RAFT-mediated, surfactant-free, *ab initio*, batch emulsion polymerization of *n*-butyl acrylate (*n*BA) and its copolymerization with methyl methacrylate (MMA) were studied. The control agent was a surface-active trithiocarbonate macromolecular RAFT agent composed of a hydrophilic poly(ethylene oxide) (PEO) block and a hydrophobic dodecyl chain. The homopolymerizations of *n*BA were fast with high final conversions, and the polymer chains were well-controlled with narrow molar mass distribution. The length of the PEO chain was shown to affect the particle size and the polymerization kinetics directly. We found the conditions to tune the particle size independently from the poly(*n*-butyl acrylate) chain length by playing with a mixture of macro-RAFT agents with long and short PEO segment or by adding a PEO-based nonionic surfactant. The copolymerizations of *n*BA and MMA exhibited features very similar to those of the *n*BA homopolymerizations provided that the molar percentage of MMA did not exceed approximately 75%. In all cases, stable, submicrometric particles composed of amphiphilic diblock copolymer chains were formed.

Introduction

The development of controlled/living radical polymerization (CRP) techniques^{1,2} opened a new era in the domain of polymer chemistry. One of the main advantages is the possibility to design a broad variety of macromolecular architectures that are not accessible via other polymerization methods.^{3,4} For this purpose, the RAFT (reversible addition–fragmentation chain transfer) technique based on the use of thiocarbonylthio chain transfer agents is quite simple and efficient.^{5,6} Another advantage of CRP is the possibility of applying different processes because the radical polymerization is not restricted to homogeneous conditions, that is, bulk or solution. In particular, the most interesting process from both industrial and environmental viewpoints is the aqueous emulsion polymerization,^{7,8} which is characterized by high reaction rates and high conversions. The method leads to an aqueous suspension of submicrometric polymer particles, usually stabilized by traditional low-molar-mass, anionic or nonionic surfactants. The so-formed latex exhibits low viscosity in comparison with a polymer solution of similar solids content. It may be applied directly using adapted formulation, or it may be considered to be a convenient medium from which the polymer is further isolated. Because RAFT differs from conventional radical polymerization by the simple addition of a reversible chain transfer agent, it was initially supposed that the application of the method to aqueous emulsion polymerization would be quite straightforward. This was, however, without considering the fact that nucleation is a complex mechanism that is not independent from chain growth. In consequence, most of the attempts failed and, for a long period of time, RAFT was developed under miniemulsion polymerization conditions with

hydrophobic RAFT agents.^{9–11} Thanks to droplet nucleation and to direct location of the RAFT agent in the polymerization loci, the particle formation step was disconnected from the chain growth process, and the polymerization did not behave very differently from a bulk system.^{9–11} In this way, control over macromolecular architectures was successfully achieved in stable latexes, although problems like rate retardation and colloidal stability issues were sometimes encountered. Those difficulties were mainly related to the reactivity and solubility of the RAFT agent as well as to the nature of the selected surfactant. In miniemulsion, the recent application of a surface-active macro-RAFT agent in a surfactant-free system represented a new step in the field.¹² The first development of RAFT in a true emulsion polymerization process was first proposed by Hawket and Gilbert.^{13–16} Their strategy (also applied by Klumperman et al.¹⁷) relied on the use of a trithiocarbonate RAFT agent and on the *in situ* formation of an amphiphilic reactive diblock copolymer self-assembling into micelles. Via a slow feed of monomer, the polymerization was conducted in the absence of monomer droplets, which might otherwise cause loss of control. The polymerization was free of added low-molar-mass surfactant and could be controlled by the RAFT moiety present at the end of the hydrophobic block. More recently, surfactant-free, batch emulsion polymerization was considered, again with trithiocarbonate RAFT agents possessing a hydrophilic polymer segment for particle stabilization.^{18–20} (Note that in ref 19, ultrasonication was employed before polymerization, like in miniemulsion.) From those works and from previous unsuccessful attempts using dithiobenzoate RAFT agents,^{21–23} (i.e., good colloidal stability but poor control of the chain growth process), it was concluded that a judicious choice of the reactive group in the reversible chain transfer agent along with the proper hydrophilic/hydrophobic balance were required for conducting successfully

*Corresponding author: E-mail: bernadette.charleux@upmc.fr.

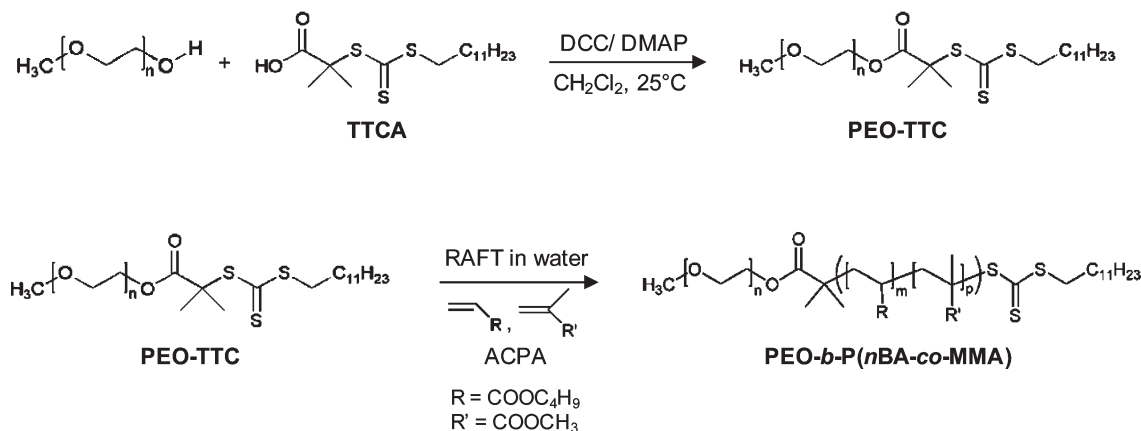


Figure 1. Synthesis of the PEO-TTC macro-RAFT agents from 2-(dodecylthiocarbonothioylthio)-2-methylpropanoic acid (TTCA) and their use in the controlled radical homopolymerization of *n*-butyl acrylate (*n*BA) and the copolymerization of *n*BA with methyl methacrylate (MMA) in aqueous emulsion. DCC is *N,N*-dicyclohexylcarbodiimide, DMAP is 4-(dimethylamino)pyridine, and ACPA is 4,4'-azobis(4-cyanopentanoic acid).

surfactant-free, *ab initio*, batch emulsion polymerization controlled by RAFT. For this purpose, the best suited RAFT agents to obtain a good control of the particle size and of the polymer chain architecture at the same time are indeed based on amphiphilic trithiocarbonates.

2-(Dodecylthiocarbonothioylthio)-2-methylpropanoic acid (TTCA) is a widely employed trithiocarbonate RAFT agent (Figure 1) that is known for efficiently controlling the polymerization of a large variety of monosubstituted ethylenic monomers under homogeneous conditions.²⁴ Thanks to its amphiphilic properties at alkaline pH, it could recently be successfully employed as both a surfactant and a control agent for the batch emulsion copolymerization of *n*-butyl methacrylate (*n*BMA) with *n*-butyl acrylate (*n*BA) or styrene.²⁵ Stable latexes of 50 to 150 nm in diameter were obtained. The number-average molar masses, M_n , of the polymer chains were close to the expected values, with polydispersity indexes (M_w/M_n) ranging from 1.4 to 2.0. In the respective homopolymerizations of styrene or *n*BMA, the polymerizations were either extremely slow (styrene) or not controlled (*n*BMA). Our approach to reach autostabilized polystyrene (PS) or poly(*n*-butyl acrylate) (P*n*BA) latex particles composed of controlled polymer chains formed via aqueous emulsion polymerization consisted of substituting the carboxylic group by a hydrophilic poly(ethylene oxide) (PEO) chain to create an amphiphilic PEO macro-RAFT agent (PEO-TTC, Figure 1).^{20,26} The latter exhibits a structure very close to that of the nonionic surfactants classically used in emulsion polymerization, for example, Brij35. The amphiphilic macro-RAFT agent PEO2K-TTC (where 2K denotes a PEO chain length of 2 kg mol⁻¹) showed great promise in the batch emulsion homopolymerization of *n*BA and styrene by acting as both the surfactant and the RAFT agent.²⁰ So far, it can be considered to be the most effective macro-RAFT agent for surfactant-free, *ab initio*, batch emulsion polymerization. Moreover, its application to such an aqueous process is a way of producing PEO-based amphiphilic block copolymers without organic solvents.

The purpose of this work was to better understand the properties of the PEO-TTC macro-RAFT agent and to expand its application to new polymerization systems. We were first interested in testing the influence of the PEO chain length on the particle formation and stability and on the control over the homopolymerization of *n*BA. Our aim was to find appropriate conditions to tune the particle size efficiently and to maintain small particles and good stability even when high molar masses were targeted. Then, the PEO2K-TTC was further tested in the copolymerization of *n*BA with methyl methacrylate (MMA) to check its efficiency for controlling the synthesis of all-acrylate

polymers that find broad application in industry, for example, for coating or adhesive applications or as reinforcing materials. In a more general way, the purpose of this work was to demonstrate the great potential and nearly universal character of the PEO-TTC macro-RAFT agents for polymerization in aqueous dispersed systems.

Experimental Section

Materials. MMA (99%, Aldrich) and *n*BA (>99%, Aldrich) were distilled under reduced pressure before use. 4,4'-Azobis(4-cyanopentanoic acid) (ACPA, >98%, Fluka), sodium hydrogencarbonate (NaHCO₃, >99.7%, Aldrich), Brij35 (PEO-C₁₂H₂₅, M_n = 1.2 kg mol⁻¹), and sodium dodecyl sulfate (SDS, Aldrich 98%) were used as received. Deionized water was used for all polymerizations. The poly(ethylene oxide) trithiocarbonate macro-RAFT agent PEO2K-TTC was synthesized from α -methoxy ω -hydroxy poly(ethylene oxide) (M_n = 2 kg mol⁻¹, Fluka) and TTCA, as detailed before.²⁰ PEO1K-TTC (M_n of the PEO block = 1 kg mol⁻¹, Fluka) and PEO5K-TTC (M_n of the PEO block = 5 kg mol⁻¹, Fluka) were synthesized accordingly with 2 or 20 equiv of TTCA, respectively. (See the Supporting Information for a detailed description of the synthesis and characterization.)

Reversible Addition–Fragmentation Chain Transfer-Mediated Emulsion Homopolymerization of *n*-Butyl Acrylate. In a typical experiment (Table 1, entry A2), 0.203 g of PEO2K-TTC (8.41×10^{-5} mol) was dissolved in 8.80 g of deionized water. Then, 0.49 mL (3.0 mg, 1.1×10^{-5} mol) of a stock solution of ACPA in water (concentration = 6.1 mg mL⁻¹ neutralized by 3.5 molar equiv of NaHCO₃) and 1.404 g (1.10×10^{-2} mol) of *n*BA were added. After deoxygenation by bubbling with nitrogen for 30 min in iced water, the sealed flask containing the reaction mixture was immersed in an oil bath thermostatted at 70 °C. Samples were periodically withdrawn to monitor the conversion by gravimetry, the evolution of the average particle diameter, and the number-average molar mass, M_n , of the polymer with conversion. Polymerizations were quenched by immersion of the samples in iced water.

Reversible Addition–Fragmentation Chain Transfer-Mediated Emulsion Copolymerization of *n*-Butyl Acrylate and Methyl Methacrylate. A typical recipe using PEO2K-TTC as both the surfactant and the RAFT agent is as follows (Table 2, entry AM2): 0.167 g of PEO2K-TTC (6.9×10^{-5} mol) was dissolved in 3.670 g of deionized water. Then, 0.50 mL (4.0 mg, 1.4×10^{-5} mol) of a stock solution of ACPA in water (concentration = 8.0 mg mL⁻¹ neutralized by 3.5 molar equiv of NaHCO₃), 0.575 g (4.5×10^{-3} mol) of *n*BA, and 0.459 g of MMA (4.6×10^{-3} mol) were added. After deoxygenation by bubbling with nitrogen for 30 min in iced water, the sealed flask containing the reaction mixture was immersed in an

Table 1. Macromolecular and Colloidal Characteristics of the Polymer Latexes Prepared via *ab Initio* Batch Emulsion Homopolymerization of *n*-Butyl Acrylate (*n*BA) in the Presence of PEO-TTC Macro-RAFT Agents with Different Poly(ethylene oxide) (PEO) Chain Length at 70 °C^a

expt	wt % monomer in the latex	RAFT agent ^a	[PEO-TTC] ₀ (mmol L _{H₂O} ⁻¹)	[ACPA] ₀ (mmol L _{H₂O} ⁻¹) ^b	[<i>n</i> BA] ₀ /[PEO- TTC] ₀	time (h)	conv. (%) ^c	<i>M</i> _{n,theor} (kg mol ⁻¹) ^d	<i>M</i> _{n,exptl} (kg mol ⁻¹) ^e	<i>M</i> _w / <i>M</i> _n ^e	<i>D</i> _z (nm); (poly) ^f
A1	13	1K	9.1	1.2	129	5.2	97	17.5	multimodal	multimodal	340 (0.19)
A2	13	2K	9.1	1.2	130	3.6	90	17.4	18.4	1.11	184 (0.02)
A3	13	5K	9.3	1.2	130	2.2	90	20.5	18.3	1.48	71 (0.10)
A4	24	2K	9.5	2.0	262	3.7	96	34.6	33.8	1.24	510 (0.09) ^g
A5	23	2K + 5K	7.7 (2K) + 1.7 (5K)	1.7	254	1.6	90	32.2	34.2	1.22	209 (0.07)
A6	24	2K + 5K	5.2 (2K) + 4.3 (5K)	1.5	263	2.9	99	35.3	35.7	1.35	215 (0.05)
A7	24	2K + Brij35	4.7 + 5.0 (Brij35)	1.0	521	1.8	52	21.3	20.1	1.30	115 (0.08)
A8	24	2K + Brij35	2.7 + 4.8 (Brij35)	0.5	891	2.5	98	36.8	32.8	1.30	122 (0.07)
						2.0	79	54.9	61.1	1.26	240 (0.06)
						3.5	94	63.5	85.4	1.41 ^h	250 (0.03)
						2.9	77	90.1	114.8	1.20	296 (0.11)
						5.5	92	107.3	130.4	1.49 ^h	307 (0.03)

^a PEO-TTC is the macro-RAFT agent derived from TTCA, where 1K, 2K, and 5K denote the corresponding PEO chain length with *M*_n(PEO) = 1 kg mol⁻¹ ("1K"), 2 kg mol⁻¹ ("2K"), and 5 kg mol⁻¹ ("5K"). ^b ACPA (4,4'-azobis-4-cyanopentanoic acid) was neutralized by 3.5 mol equiv of NaHCO₃. ^c Monomer conversion was determined by gravimetry. ^d Theoretical number-average molar mass at the experimentally determined conversion. ^e Number-average molar mass (*M*_n) and polydispersity index (*M*_w/*M*_n) determined by SEC with polystyrene (PS) calibration. ^f *D*_z is the average particle diameter from dynamic light scattering analysis (the lower the dispersity factor, poly, the narrower the particle size distribution). ^g 5.5 wt % of precipitate based on the total polymer mass. ^h Shoulder on the high molar mass side of the peak.

oil bath thermostatted at 70 °C. Samples were periodically withdrawn to monitor the conversion by gravimetry, the evolution of the average particle diameter, and the number-average molar mass, *M*_n, of the polymer with conversion. Polymerizations were quenched by immersion of the samples in ice water.

Characterization Techniques. The purity of the RAFT agents was determined by ¹H NMR spectroscopy in CDCl₃ at room temperature (300 and 500 MHz Bruker). (For details, see the Supporting Information.)

Size exclusion chromatography was performed at 40 °C with two columns (PSS SDV, linear MU, 8×300 mm²; bead diameter: 5 μm; separation limits: 400 to (2×10⁶) g mol⁻¹). Tetrahydrofuran (THF) was used as the eluent at a flow rate of 1 mL min⁻¹. A differential refractive index detector (LDC Analytical refractometer IV) was used, and molar masses (*M*_n), the number-average molar mass, *M*_w, the weight-average molar mass, and PDI = *M*_w/*M*_n, the polydispersity index) were derived from a calibration curve based on PS or poly(methyl methacrylate) (PMMA) standards from Polymer Standards Service. In all plots showing the evolution of *M*_n with monomer conversion, the straight line corresponds to the expected evolution of the theoretical value *M*_{n,theor}, calculated by the ratio of the initial mass of monomer multiplied by the overall weight conversion over the initial mole number of the macro-RAFT agent plus the molar mass of the latter.

The *z*-average particle diameter (*D*_z) and polydispersity factor (poly) of the diluted aqueous dispersions were measured by dynamic light scattering (DLS) at a temperature of 25 °C at 90°, with a Zetasizer Nano S90 from Malvern using a 5 mW He–Ne laser at 633 nm. The measurements were performed directly after polymerization and then after a storage period of 2 months at 4 °C.

Cryo-transmission electron microscopy (cryo-TEM) was used to determine the morphology and size of the polymer nanoparticles. According to protocols reported elsewhere,^{27,28} thin liquid films of particle dispersions (0.4 wt % solids content) were flash frozen in liquid ethane and observed at –180 °C on a JEOL JEM-2100 LaB₆ microscope (Cs = 2.0 mm) operating at 200 kV under low-dose conditions (10 electrons Å⁻² s⁻¹) at a nominal magnification of 20 000 and 40 000 with a 1.5 to 2.0 μm defocus range. Digital images were recorded on a Gatan Ultra-scan 1000 CCD camera.

Results and Discussion

Surfactant-Free, Batch, Emulsion Homopolymerization of *n*-Butyl Acrylate in the Presence of PEO-TTC with Different Chain Lengths. Besides the already tested PEO2K-TTC,²⁰

two additional PEO-macro-RAFT agents differing in the length of the PEO chain have been synthesized in order to (i) prepare PEO-*b*-P*n*BA diblock copolymers of different PEO chain length and (ii) study the influence of the PEO length on the size and stability of the latex particles. PEO1K-TTC (with *M*_n(PEO) = 1 kg mol⁻¹) and PEO5K-TTC (with *M*_n(PEO) = 5 kg mol⁻¹) were thus employed in the emulsion polymerization of *n*BA under the same experimental conditions as those in ref 20. In the presence of the macro-RAFT agent PEO1K-TTC with the shortest PEO chain, big particles (*D*_z = 340 nm) of rather broad size distribution (DLS polydispersity factor = 0.19) were formed (Table 1, experiment A1). The presence of some aggregates (in the micrometer range, 2% in intensity from DLS analysis) was also observed. With PEO2K-TTC (experiment A2), the particle size drastically decreased (*D*_z = 184 nm) and the distribution became much narrower, as already reported in our previous work.²⁰ When PEO5K-TTC with the longest PEO chain was used (experiment A3), very small particles of 71 nm in diameter rapidly formed. Therefore, comparing the three macro-RAFT agents, one can conclude that the longer the stabilizing PEO block was (larger weight content of PEO at similar molar concentration: 7 wt % for A1, 12 wt % for A2, and 24 wt % for A3 based on the overall weight of macro-RAFT agent and polymer), the smaller the formed particles were. This observation is not surprising and has already been reported for conventional emulsion polymerization in the presence of nonionic surfactants.²⁹ In addition, the latex stability over time was good because the diameter did not significantly change after 2 months of storage. In relation to the lower particle size and hence larger particle number, the kinetics were significantly different (Figure 2) and the polymerization was faster when the length of the stabilizer was increased. Those effects on particle size and polymerization kinetics clearly show that although they are reactive species the PEO-TTC macro-RAFT agents act similarly to classical nonionic surfactants for nucleation and latex stabilization.

Regarding the polymer chain characteristics, poor control was achieved with PEO1K-TTC (which, however, was highly efficient in the solution polymerization of *n*BA in 1,4-dioxane; see Table SI-1 and Figure SI-2a in the Supporting Information). The SEC traces were multimodal all over the polymerization, indicating the presence of a mixture of unreacted macro-RAFT agent, of PEO-*b*-P*n*BA block

Table 2. Macromolecular and Colloidal Characteristics of the Polymer Latexes Prepared in the Absence of Surfactant via Ab initio Batch Emulsion Copolymerization of *n*-Butyl Acrylate (*n*BA) and Methyl Methacrylate (MMA) in the Presence of PEO2K-TTC as a Macromolecular RAFT Agent at 70 °C^a

expt ^a	wt % monomer in latex	<i>n</i> BA/MMA molar ratio	[PEO2K-TTC] ₀ (mmol L ⁻¹ H ₂ O ⁻¹)	[ACPA] ₀ (mmol L ⁻¹ H ₂ O ⁻¹) ^b	[monomer(s)] ₀ / [PEO2K-TTC] ₀	time (h)	conv. (%) ^c	<i>M</i> _{n,theor} (kg mol ⁻¹) ^d	<i>M</i> _{n,exptl} (PS) (kg mol ⁻¹) ^e	<i>M</i> _{n,exptl} (PMMA) (kg mol ⁻¹) ^f	<i>M</i> _w / <i>M</i> _n (PS) ^g	<i>D</i> _z (nm); (poly) ^g
A9	23	100/0	19.2	4.0	130	5.1	99	18.8	18.9	20.0	1.21	220 (0.02)
AM1	22	74/26	18.7	3.8	133	6.1	94	17.6	17.6	19.4	1.33	174 (0.08)
AM2	21	50/50	18.8	3.9	131	5.4	92	16.2	16.9	17.7	1.12	125 (0.04)
AM3	33	50/50	38.4	8.2	130	6.1	97	16.6	15.9	17.4	1.33 ^h	139 (0.06)
AM4	20	25/75	18.8	4.0	133	6.1	91	15.5	14.3	15.7	1.26	155 (0.06)
AM5	33	25/75	38.4	8.2	130	3.2	66	12.7	8.3	9.0	1.22	81 (0.28) ⁱ
AM6	20	10/90	19.0	4.4	131	3.8	>71	12.0	9.7	11.0	1.68	1600 (75%) + 300 (25%) (0.48) ⁱ
M1	19	0/100	17.8	3.9	140	5.3	>79	16.7	multimodal			not stable

^a PEO2K-TTC is the macro-RAFT agent derived from TTCA, where 2K designates the poly(ethylene oxide) (PEO) chain length with *M*_n(PEO) = 2 kg mol⁻¹. ^b ACPA (4,4'-azobis(4-cyanopentanoic acid) was neutralized by 3.5 mol equiv of NaHCO₃. ^c Monomer conversion was determined by gravimetry. ^d Theoretical number-average molar mass at the experimentally determined conversion. ^e Number-average molar mass (*M*_n) and polydispersity index (*M*_w/*M*_n) determined by SEC with polystyrene calibration. ^f Number-average molar mass (*M*_n) and polydispersity index (*M*_w/*M*_n) determined by SEC with poly(methyl methacrylate) calibration. ^g *D*_z is the average particle diameter from dynamic light scattering analysis (the lower the polydispersity factor, poly, the narrower the particle size distribution). ^h Size exclusion chromatogram shows a shoulder on the low molar mass side of the peak. ⁱ Viscous latex. The presence of 1 to 2 μm aggregates was observed by DLS.

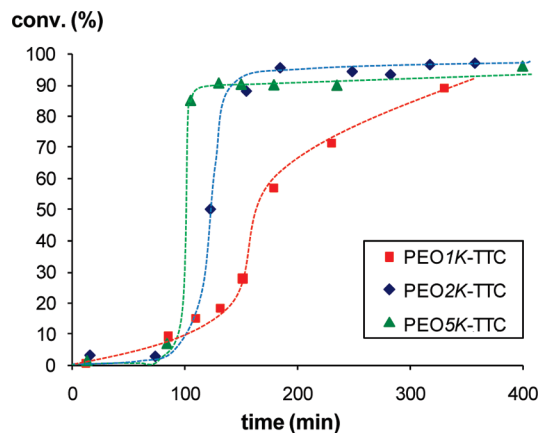


Figure 2. Evolution of the monomer conversion versus time for the aqueous emulsion polymerization of *n*BA at 70 °C in the presence of PEO1K-TTC (■), PEO2K-TTC (◆), and PEO5K-TTC (▲).

copolymer and of noncontrolled P*n*BA homopolymer (Figure SI-3a in the Supporting Information). The poor control of the polymerization is probably related to the heterogeneity of particle size. One possible explanation might be found in the enhanced hydrophobicity of the PEO1K-TTC leading to larger solubility in the monomer phase and poorer particle stabilization. In contrast, with the longer PEO2K-TTC, the control over the polymer chain growth was particularly good with narrow molar mass distribution and good match between the experimental and theoretically expected *M*_n values. Similarly, in the presence of PEO5K-TTC, the experimentally determined molar mass matched the theoretical value quite well. The polydispersity index, however, was larger (*M*_w/*M*_n = 1.48) than that with PEO2K-TTC (*M*_w/*M*_n = 1.11), which must be partially attributed to the limited efficiency of the macro-RAFT agent (Figure SI-3b in the Supporting Information). The same observation was made in solution and might be ascribed to the presence of a low amount (≤15%) of unfunctionalized PEO (Table SI-1 and Figure SI-2b in the Supporting Information).

The size and stability of the latex particles strongly depended on the length of the hydrophobic P*n*BA block formed in situ, which was directly determined by the initial *n*BA/PEO-TTC molar ratio used and thus related to the concentration of the “reactive surfactant” in the initial polymerization medium.²⁰ When rather high solids contents such as 24 wt % were targeted (wt % of *n*BA, given by the mass of monomer related to the total mass of the initial reaction medium), a compromise between the maximum length of the P*n*BA (low macro-RAFT agent concentration) and the stability of the system (need for sufficient stabilizer concentration) must be found. Entry A4 in Table 1 is such a limit case, where very large particles were obtained for rather high P*n*BA chain length. (See the discussion in our previous publication.²⁰) To enhance the latex stability at this solids content and to diminish the particle size without adding free, “non-reactive” surfactant, part of the PEO2K-TTC was replaced by PEO5K-TTC. Experiment A4 was thus repeated in the presence of PEO2K-TTC mixed with 18 mol % of PEO5K-TTC (with respect to the overall reactive surfactant) (Table 1, entry A5). Under comparable experimental conditions, the presence of 18 mol % of PEO5K-TTC, bearing longer hydrophilic PEO chains, clearly led to a very significant change in particle diameter because it was more than halved (215 vs 510 nm), and no aggregates were detected. In experiment A6 (Table 1), the molar proportion of PEO5K-TTC was further increased to 45 mol % while keeping the

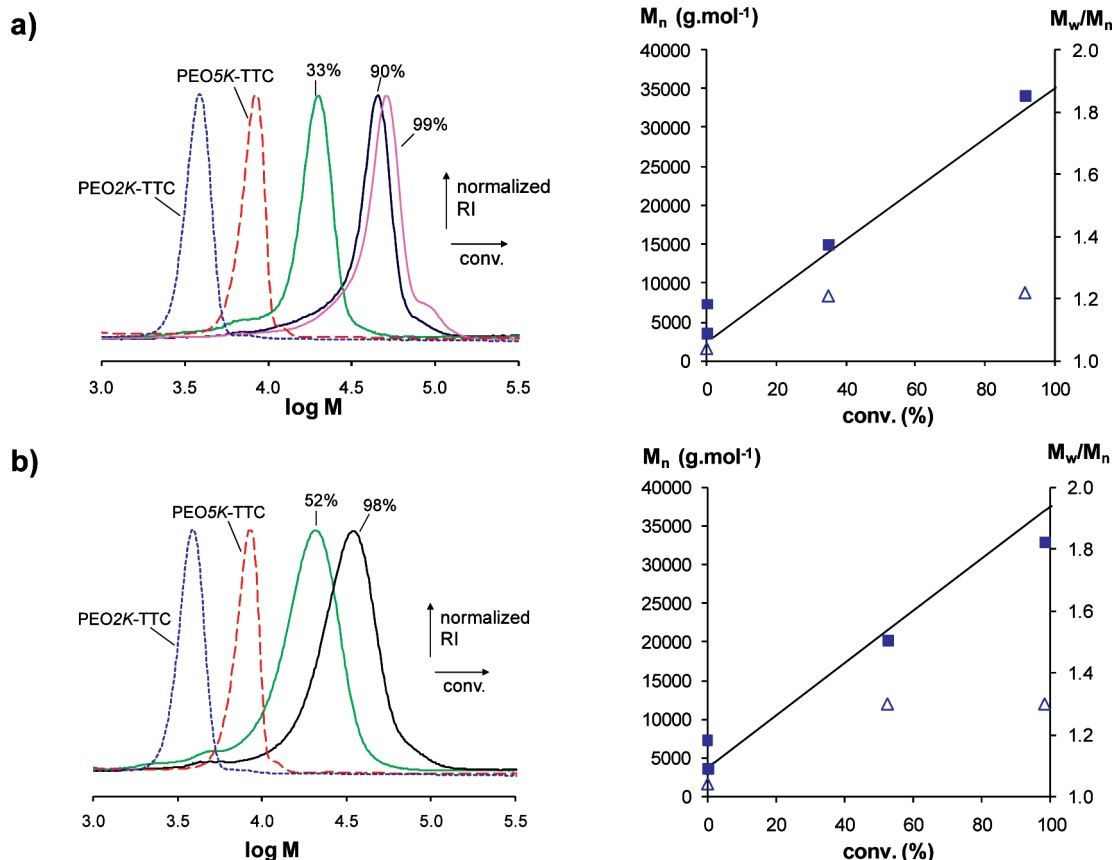


Figure 3. Aqueous emulsion polymerization of *n*BA in the presence of mixtures of PEO2K-TTC and PEO5K-TTC. Evolution of the size exclusion chromatograms with monomer conversion and evolution of the number-average molar mass (M_n) (■) and polydispersity index (M_w/M_n) (Δ) versus monomer conversion for (a) experiment A5 performed with 18 mol % and (b) experiment A6 performed with 45 mol % of PEO5K-TTC. The straight lines correspond to the theoretically expected M_n versus conversion.

monomer/RAFT agent molar ratio constant. The particle size then decreased to 122 nm, and a narrow particle size distribution was preserved. The size exclusion chromatograms for different conversions were narrow (Figure 3), showing a slight tailing toward the lower molar mass side. Experimental M_n matched the theoretical values quite well, indicating a good overall efficiency of the macro-RAFT agents. The substitution of a fraction of PEO2K-TTC by a macro-RAFT agent with longer PEO chain length is thus a means to tune the particle size without changing the target molar mass.

Emulsion polymerizations of *n*BA with PEO2K-TTC were also performed in the presence of a conventional surfactant at relatively high initial monomer contents (24 wt %) to achieve stable latexes composed of PEO-*b*-P*n*BA chains of higher molar mass (compared with experiments where PEO2K-TTC was used as both the surfactant and the control agent) without altering the particle size or destabilizing the latex. A preliminary experiment (not shown) was performed under the same conditions as experiment A5 but in the presence of an anionic surfactant, sodium dodecyl sulfate. Monomer conversion was low after 5 h (<60%), and the formed latex particles were not stable. Moreover, SEC revealed no control over the polymerization. Further experiments (A7 and A8) were thus performed in the presence of a nonionic surfactant, Brij35, a polyoxyethyleneglycol dodecyl ether with $n(\text{EO}) = 23$ ($M_n = 1.2 \text{ kg mol}^{-1}$), exhibiting a critical micelle concentration³⁰ of $4 \times 10^{-4} \text{ mol L}^{-1}$ and whose amphiphilic structure resembles that of PEO1K-TTC. When equimolar amounts of PEO2K-TTC and Brij35 were used (Table 1, experiment A7), stable latex particles were

obtained with a diameter half that of particles formed in the reference experiment A4 (250 vs 510 nm), although the monomer/RAFT agent ratio was double.²⁹ This means that better stability was reached in the presence of the nonreactive surfactant (Brij35), although the overall PEO weight percentage in experiment A4 was larger than that in experiment A7 (1.7 vs 1.3 wt % in the latex). This might be explained by a more efficient location of the latter at the particle surface, even at high conversion, in contrast with the PEO segments attached to a polymer chain that may be buried in the particle core upon chain extension. Finally, (Table 1, experiment A8) hydrophobic chains of higher M_n , above $100\,000 \text{ g mol}^{-1}$, were targeted (*n*BA/RAFT ≈ 900) at Brij35 and monomer concentrations similar to those used in experiment A7. Again, stable latex particles were formed of slightly bigger dimension ($\sim 300 \text{ nm}$ in diameter). For both experiments (A7 and A8), monomer conversion was high (>90%) within short times, and the experimentally determined M_n matched the theoretical values well. Throughout the polymerization, SEC traces were essentially symmetric and narrow. However, for monomer conversions above 80% a shoulder at the higher molar mass side was observed, as is often seen in the polymerization of acrylate monomers controlled via RAFT.

In conclusion, with PEO2K-TTC and PEO5K-TTC, the RAFT-mediated radical emulsion polymerization systems formed self-stabilized particles composed of well-defined amphiphilic PEO-*b*-P*n*BA diblock copolymer chains. Their efficiency as RAFT agents as well as stabilizers is thus clearly demonstrated, indicating the absence of water-soluble free chains in the latex aqueous phase. In addition, mixing both

chain transfer agents allowed us to tune the particle size independently from the molar mass of the hydrophobic P*n*BA block. Moreover, in the presence of an additional surfactant with similar structure and at low concentration of the RAFT agent, very high molar mass could be achieved in stable latexes. Besides the possibility of forming well-defined polymer colloids, this emulsion polymerization procedure is also a way to synthesize PEO-*b*-P*n*BA amphiphilic diblock copolymers in solvent-free systems with the additional advantage of a fast polymerization reaction in comparison with homogeneous conditions.

Surfactant-Free, Batch Emulsion Copolymerization of *n*-Butyl Acrylate and Methyl Methacrylate in the Presence of PEO2K-TTC. We investigated the emulsion copolymerization of *n*BA with MMA in the presence of PEO2K-TTC to enlarge the spectrum of polymerizable monomers and to prepare latexes of amphiphilic PEO-*b*-P(*n*BA-*co*-MMA) block copolymers (Figure 1). It should be noted that TTCA does not control the homopolymerization of methacrylates because the leaving/initiating radical is not stable enough compared with the propagating methacrylic radical. As reported recently, it was possible to control the emulsion

polymerization of a methacrylic ester monomer, namely, *n*BMA using TTCA, by adding a small percentage of styrene (≥ 7 mol %) or *n*BA (14 mol %). Thanks to the presence of *n*BA- or styryl-terminated propagating radicals, the transfer reaction for the copolymerization was improved, and the chain growth was well-controlled.²⁵ The same conclusions should thus hold with our PEO-TTC macro-RAFT agents directly derived from TTCA.

The emulsion copolymerization of *n*BA and MMA was tested at *n*BA/MMA molar ratios of 74/26, 50/50, 25/75, and 10/90 and constant monomer (2.5 mol L^{-1} corresponding to about 20 wt % solids), PEO2K-TTC (19 mmol L^{-1}), and initiator (4 mmol L^{-1}) concentrations (Table 2, entries AM1, AM2, AM4, and AM6). The kinetics for the copolymerizations and for the corresponding homopolymerizations of both *n*BA (experiment A9) and MMA (experiment M1) are presented in Figure 4. For all monomer ratios (except *n*BA/MMA = 10/90), high monomer conversions were reached within 5 h ($> 90\%$). As already observed for the homopolymerization of *n*BA (in this work and in ref 20), the copolymerizations with an *n*BA/MMA molar ratio of 74/26, 50/50, and 25/75 started after an induction period of about 60 min. This induction period was not observed for the homopolymerization of MMA or for the copolymerization of *n*BA/MMA at high MMA content (*n*BA/MMA molar ratio = 10/90), which must be attributed to the low efficiency of the RAFT agent for methacrylates. Similarly, in the *n*BMA/styrene system reported earlier,²⁵ no induction period was observed for the emulsion homopolymerization of *n*BMA, but the presence of styrene, however, led to a pronounced inhibition period depending on the amount of styrene. (For instance, it was about 3 h for 7 mol % of styrene.)

The copolymerizations of *n*BA/MMA at molar ratios equal or superior to 25/75 led to stable latexes with particle diameter in the range of 100 to 200 nm. A minimum diameter of 125 nm was obtained for equal molar ratios of both monomers (experiment AM2). It should also be noted that an increase in viscosity was observed for MMA contents higher than 75%, with, in addition, an increase in particle size and a broadening of the particle size distribution. For the homopolymerization of MMA in the presence of PEO2K-TTC (entry M1, Table 2), the formed latex was not stable. A possible explanation might be found in the rather hydrophilic character of PMMA and its miscibility with PEO, which might impede proper

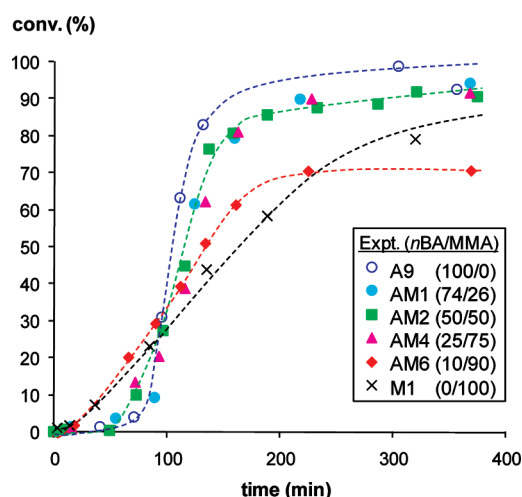


Figure 4. Evolution of the monomer conversion versus time for the aqueous emulsion (co)polymerizations of *n*-butyl acrylate (*n*BA) with various amounts of methyl methacrylate (MMA) at 70 °C (monomer conversion determined by gravimetry).

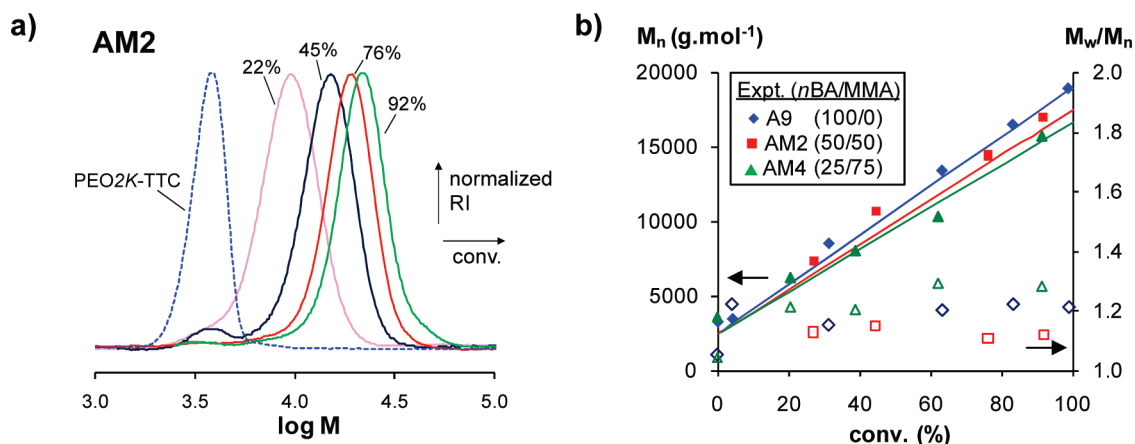


Figure 5. Surfactant-free, batch emulsion homopolymerization of *n*-butyl acrylate (*n*BA) and copolymerizations of *n*BA with methyl methacrylate (MMA) (molar ratio 50/50 and 25/75) in water at 70 °C: (a) evolution of the size exclusion chromatograms with conversion for the experiment using equimolar amounts of *n*BA and MMA (50/50) (Table 2, entry AM2); (b) number-average molar mass, M_n , and polydispersity index, M_w/M_n , determined by size exclusion chromatography versus conversion. (PS calibration was used for the experiments using 100 and 50% of *n*BA, and PMMA calibration was used for the experiment with 75% MMA.) The straight lines correspond to the theoretically expected M_n versus conversion.

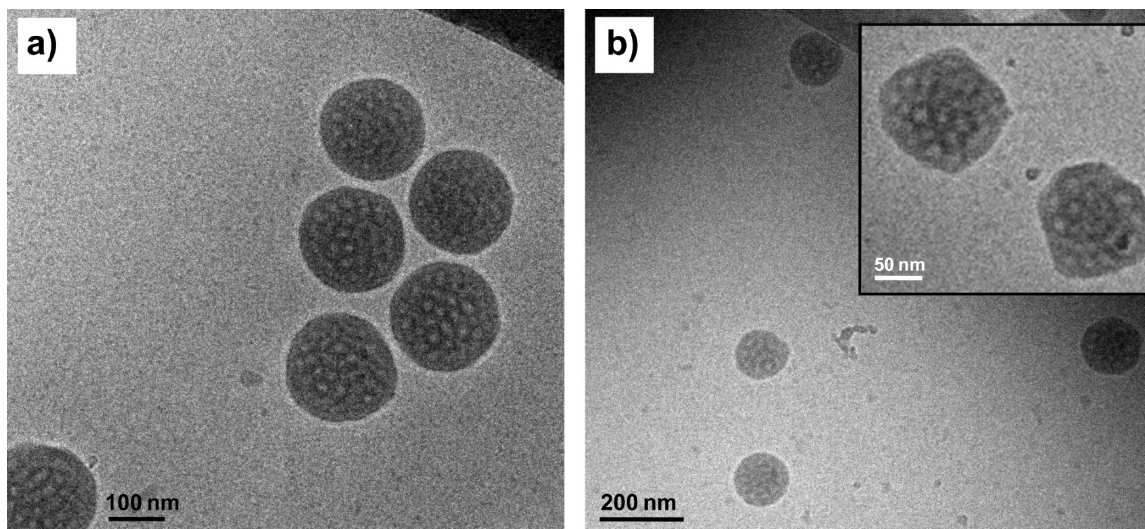


Figure 6. Cryo-TEM micrographs of particles obtained in (a) experiment **A9** (100% *n*BA) and (b) experiment **AM4** (*n*BA/MMA = 25/75) (panoramic view and detail).

phase separation, that would lead to small, well-defined particles.

Apart from the homopolymerization of MMA, which was not controlled, the size exclusion chromatograms at various monomer conversions were generally narrow and symmetric. Figure 5a shows the shift of the SEC traces with conversions for the experiment **AM2** using equal amounts of *n*BA and MMA and the absence of residual macro-RAFT agent above 45% conversion. For all *n*BA/MMA molar ratios investigated here, M_n increased linearly with monomer conversion, exhibiting good agreement with the theoretical values and low M_w/M_n (Figure 5b). The polydispersity indexes were the lowest for the polymerization employing equimolar amounts of both monomers.

Those results show that self-stabilized particles composed of well-defined PEO-*b*-P(*n*BA-*co*-MMA) diblock copolymers could be successfully synthesized at relatively high monomer contents, up to 24 wt %. To reach higher solids contents, additional experiments were performed at 33 wt % of monomer (Table 2, entries **AM3** and **AM5**). For the experiment **AM3** (*n*BA/MMA = 50/50), a stable latex was obtained, and the particle diameter increased with respect to experiment **AM2**. Concerning the control of the polymerization, the determined molar masses remained close to the expected ones; however, M_w/M_n increased, and a shoulder at the low molar masses side appeared. For *n*BA/MMA = 25/75 (**AM5**), a viscous latex with poor stability was formed, similar to the one obtained for the homopolymerization of MMA in the presence of PEO2K-TTC (**M1**).

It can thus be concluded that the copolymerization of MMA with *n*BA can be controlled over a broad composition range in an emulsion process at rather high solids contents in the presence of PEO2K-TTC. Because of the higher water solubility of MMA compared with that of *n*BA and because of its higher reactivity in copolymerization,³¹ the incorporation of MMA in the formed copolymer was initially favored. Thanks to the simultaneous growth of all chains shown by the linear increase in M_n with monomer conversion, the amphiphilic block copolymers thus exhibited a gradient composition in the hydrophobic segment with narrow composition distribution.³² In classical radical copolymerization, such homogeneous composition cannot be reached in batch process but only under continuous monomer addition under starved-feed conditions.

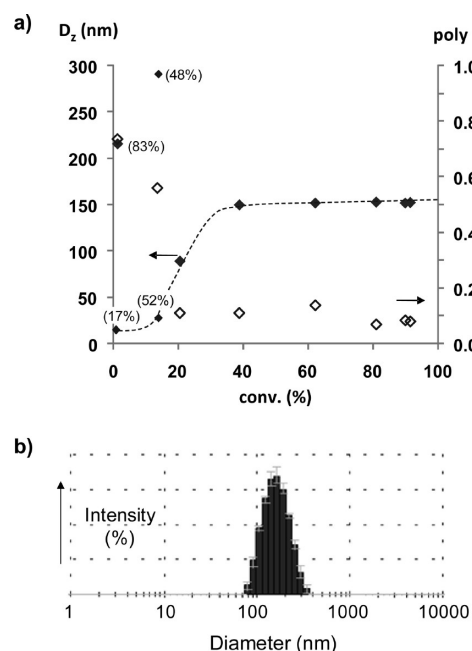


Figure 7. (a) Evolution with monomer conversion of the *z*-average particle diameter (D_z) (◆) and polydispersity factor (poly) (◇) measured by DLS for experiment **AM4** (Table 2). The values inside the brackets stand for the relative percentages by intensity of the two size populations present at low monomer conversion. (b) Final size distribution from DLS averaged on three measurements for **AM4** at 91% monomer conversion.

To observe the morphology of the copolymer particles, the final latexes **A9** (Table 2, 100% *n*BA) and **AM4** (Table 2, *n*BA/MMA = 25/75) were characterized by cryo-TEM (Figure 6). The particles were quite homogeneous in size, and no aggregates were detected. The diameter was slightly smaller than that determined by DLS, which is not unexpected considering that DLS gives a hydrodynamic diameter. Interestingly, the particles exhibited a nanostructure appearing as clear and dark zones. A possible explanation might be found in the formation of water pools in the particles induced by the presence of hydrophilic PEO chains. This was proposed and discussed by Kobayashi et al. for PS latexes prepared in the presence of nonionic

PEO-based emulsifiers.³³ It was also shown very recently in the RAFT-mediated miniemulsion polymerization of styrene using a PEO-based macro-RAFT agent.¹² In our case, however, the T_g of the polymer was lower than that of PS, in particular, for PnBA, which might be unfavorable for the stability of such multihollow structures. The existence of PEO-rich domains in the particle core might be another possibility. Potential explanations for their formation might be related either to local phase separation or to the process of nucleation. Actually, the particles shown in the expanded view of Figure 6b were not strictly spherical in shape (raspberry-like particles) and might result from the aggregation of individual smaller particles during the polymerization. Indeed, as illustrated by Figure 7a, showing the evolution of the particle size with conversion, the diameters (measured by DLS) exhibited a jump at approximately 20–30% monomer conversion, which might be attributed to limited aggregation of small-size particles (possibly, block copolymer micelles). At final conversion, one single population was observed, and no micelles could be detected (Figure 7b).

Conclusions

The surfactant-free, *ab initio*, batch emulsion polymerization of *n*BA and its copolymerization with MMA was successfully controlled via RAFT using a surface-active trithiocarbonate macro-RAFT agent exhibiting a hydrophilic PEO block and a hydrophobic dodecyl chain. The polymerizations were fast, and the final conversions were very high. The length of the PEO chain was shown to affect the particle size and the polymerization kinetics directly. We found the conditions to tune the particle size independently from the hydrophobic chain length by playing with a mixture of macro-RAFT agents with long and short PEO segment or by adding a PEO-based nonionic surfactant. The latter allowed very high molar mass to be reached with narrow molar mass distribution. The copolymerization of *n*BA with MMA exhibited features very similar to those of the *n*BA homopolymerization, provided that the molar percentage of MMA did not exceed approximately 75%. In all cases, stable particles containing amphiphilic diblock copolymer were formed. Those particles possibly resulted from the aggregation of block copolymer micelles. Deeper investigation will, however, be necessary to elucidate this particular feature. Amphiphilic PEO-TTC macro-RAFT agents are thus highly interesting for aqueous emulsion polymerization and for the design of amphiphilic block copolymers in the complete absence of organic solvent. So far, they are the most promising control agents for RAFT-mediated emulsion polymerization.

Acknowledgment. We thank Joël Belleney for ¹H NMR analysis on the 500 MHz NMR spectrometer (Bruker). We are especially grateful to Dr. Eric Larquet for the cryo-TEM analyses, which were performed with a cryo-electron microscope at the Institut de Minéralogie et de Physique des Milieux Condensés (IMPMC), UMR 7590, supported by the Centre de Compétence NanoSciences Ile de France (C'Nano IdF). G.O. acknowledges the Albert-Ludwigs University of Freiburg and the ERASMUS exchange program for his internship at the UPMC.

Supporting Information Available: Synthesis and characterization of the poly(ethylene oxide) macro-RAFT agents, PEO1K-TTC, and PEO5K-TTC; solution polymerization of *n*BA in the presence of PEO1K-TTC and PEO5K-TTC; and

SEC for the emulsion polymerizations of *n*BA in the presence of PEO1K-TTC and PEO5K-TTC. This material is available free of charge via the Internet at <http://pubs.acs.org>.

References and Notes

- (1) *Handbook of Radical Polymerization*, Matyjaszewski, K., Davis, T., Eds.; John Wiley & Sons: Hoboken, NJ, 2002.
- (2) Braunecker, W. A.; Matyjaszewski, K. *Prog. Polym. Sci.* **2007**, *32*, 93–146.
- (3) Gnanou, Y.; Taton, D. Macromolecular Engineering by Controlled/Living Radical Polymerization. In *Handbook of Radical Polymerization*; Matyjaszewski, K., Davis, T., Eds.; John Wiley & Sons: Hoboken, NJ, 2002; pp 775–844.
- (4) Synthetic Techniques. In *Macromolecular Engineering: Precise Synthesis, Materials Properties, Applications*, Matyjaszewski, K., Gnanou, Y., Leibler, L., Eds.; Wiley-VCH: Weinheim, Germany, 2007; Vol. 1.
- (5) Chiefari, J.; Chong, Y. K.; Ercole, F.; Krstina, J.; Jeffery, J.; Le, T. P. T.; Mayadunne, R. T. A.; Meijs, G. F.; Moad, C. L.; Moad, G.; Rizzardo, E.; Thang, S. H. *Macromolecules* **1998**, *31*, 5559–5562.
- (6) *Handbook of RAFT Polymerization*; Barner-Kowollik, C., Ed.; Wiley-VCH: Weinheim, Germany, 2008.
- (7) Gilbert, R. G. *Emulsion Polymerization: A Mechanistic Approach*; Academic Press: London, 1995.
- (8) *Emulsion Polymerization and Emulsion Polymers*; Lovell, P., El-Aasser, M. S., Eds.; John Wiley & Sons: Chichester, U.K., 1997.
- (9) Save, M.; Guillemeuf, Y.; Gilbert, R. G. *Aust. J. Chem.* **2006**, *59*, 693–711.
- (10) McLeary, J. B.; Klumperman, B. *Soft Matter* **2006**, *2*, 45–53.
- (11) Cunningham, M. F. *Prog. Polym. Sci.* **2008**, *33*, 365–398.
- (12) Martins, A.; Le Bris, T.; Graillet, C.; D'Agosto, F.; Lansalot, M. *Macromolecules* **2009**, *42*, 946–956.
- (13) Ferguson, C. J.; Hughes, R. J.; Pham, B. T. T.; Hawckett, B. S.; Gilbert, R. G.; Serelis, A. K.; Such, C. H. *Macromolecules* **2002**, *35*, 9243–9245.
- (14) Ferguson, C. J.; Hughes, R. J.; Nguyen, D.; Pham, B. T. T.; Gilbert, R. G.; Serelis, A. K.; Such, C. H.; Hawckett, B. S. *Macromolecules* **2005**, *38*, 2191–2204.
- (15) Sprong, E.; Leswin, J. S. K.; Lamb, D. J.; Ferguson, C. J.; Hawckett, B. S.; Pham, B. T. T.; Nguyen, D.; Such, C. H.; Serelis, A. K.; Gilbert, R. G. *Macromol. Symp.* **2006**, *231*, 84–93.
- (16) Ganeva, D. E.; Sprong, E.; De Bruyn, H.; Warr, G. G.; Such, C. H.; Hawckett, B. S. *Macromolecules* **2007**, *40*, 6181–6189.
- (17) Bozovic-Vukic, J.; Manon, H. T.; Meuldijk, J.; Koning, C.; Klumperman, B. *Macromolecules* **2007**, *40*, 7132–7139.
- (18) Fréal-Saison, S.; Save, M.; Bui, C.; Charleux, B.; Magnet, S. *Macromolecules* **2006**, *39*, 8632–8638.
- (19) Ji, J.; Yan, L.; Xie, D. *J. Polym. Sci., Part A: Polym. Chem.* **2008**, *46*, 3098–3107.
- (20) Rieger, J.; Stoffelbach, F.; Bui, C.; Alaimo, D.; Jérôme, C.; Charleux, B. *Macromolecules* **2008**, *41*, 4065–4068.
- (21) Manguian, M.; Save, M.; Charleux, B. *Macromol. Rapid Commun.* **2006**, *27*, 399–404.
- (22) Martins dos Santos, A.; Pohn, J.; Lansalot, M.; D'Agosto, F. *Macromol. Rapid Commun.* **2007**, *28*, 1325–1332.
- (23) Wi, Y.; Lee, K.; Lee, B. H.; Choe, S. *Polymer* **2008**, *49*, 5626–5635.
- (24) Lai, J. T.; Filla, D.; Shea, R. *Macromolecules* **2002**, *35*, 6754–6756.
- (25) Stoffelbach, F.; Tibiletti, L.; Rieger, J.; Charleux, B. *Macromolecules* **2008**, *41*, 7850–7856.
- (26) Rieger, J.; Grazon, C.; Charleux, B.; Alaimo, D.; Jérôme, C. *J. Polym. Sci., Part A: Polym. Chem.* **2009**, *47*, 2373–2390.
- (27) Adrian, M.; Dubochet, J.; Lepault, J.; McDowell, A. W. *Nature* **1984**, *308*, 32–36.
- (28) Dubochet, J.; Adrian, M.; Chang, J. J.; Homo, J.-C.; Lepault, J.; McDowell, A. W.; Schultz, P. *Q. Rev. Biophys.* **1988**, *21*, 129–228.
- (29) Riess, G.; Labbe, C. *Macromol. Rapid Commun.* **2004**, *25*, 401–435.
- (30) Tran, C. D.; Yu, S. J. *Colloid Interface Sci.* **2005**, *283*, 613–618.
- (31) Emilie, B.; Pichot, C.; Guillet, J. *Makromol. Chem.* **1991**, *192*, 1629–1647.
- (32) Farcet, C.; Charleux, B.; Pirri, R. *Macromol. Symp.* **2002**, *182*, 249–260.
- (33) Kobayashi, H.; Miyahara, E.; Okubo, M. *Langmuir* **2007**, *23*, 8703–8708.